Computer Aided Design of the Tube Hydroforming and Dual Hydroforming Processes

Javad Shahbazi Karami[1*], Gholamhasan Payganeh[1], Hamid Rakhodaei[2]
[1]Faculty of MechanicalEngineerig, ShahidRajaee Teacher Training University, Tehran, Iran.
[2]Mechanical Department, University of Birmingham, Birmingham, United Kingdom.
Email of Corresponding author: Shahbazi.mech@gmail.com

Abstract
This paper presents a control model of the hydroforming and the dual hydroforming process of a tube. The theoretical part includes calculations to measure the change in tube thickness through the developed process. The hydroforming and the dual hydroforming processes are simulated in the SOLIDSIMULATION software and the static and the dynamic simulations are modeled. The obtained results for the T-shape and the X-shape dies are compared and investigated. Moreover, the developed software in MATLAB calculates the process parameters. The inputs of the developed software are the maximum internal pressure and the axial feed that could be adjusted with linear and non-linear functions. Furthermore, the material of the tube, as well as the tube's parameters, such as length, thickness, and radius, must to be given to the software. However, the properties of the tube could automatically support the CAD model. The software-generated results are the applied stress, displacement, and the energy through the process. This paper deals with the control strategy model developed in thesoftware packages. The obtained results are then subsequently compared with those of several experiments.

Keywords

1. Introduction
Hydroforming is the most efficient method in regards to manufacturing low weight and cost effective parts. The most significant part in the aircraft industry is the manufacturing of a tubular shape; hence, the structure accuracy is a crucial factor [1].
Tube hydroforming (THF) has developed into an indispensable manufacturing technique in recent years and in particular, THF has become a practical method for manufacturing complex automobile parts [2]. The tubehydroforming has improved the strength and stiffness of a manufactured parts, lowered tooling costs, lessened the need for secondary operations, and closed dimensional tolerances compared to the stamping processes, all of which has led to an overall reduction of manufacturing costs [3,4]. Success of the tube hydroforming process depends on an appropriate combination of the loading curve (internal pressure and axial feed at the tube ends), material properties, and process conditions [5]. One of the key concerns is to control the deformation process in order to maximize the expansion, so that more complex shapes in various applications can be generated. Analogously, for a given shape, higher strength, lighter weight, less formable and lower cost material can be adopted [6]. The most important factor in these manufacturing techniques is to apply the hydrostatic stress in suitable positions [7]. When deformation occurs, the limiting strain depends on the measurements of the hydrostatic stress. High level of hydrostatic pressure delays the expansion of deformation [8, 9].

The numerical method was presentedin order to anticipate process failure, which could occur through buckling, wrinkling, and bursting, based on the force balance analysis [10]. All the mentioned methods of failure directly depend on measurements of the internal pressure and the axial force [11]. The tensile tests were designed in order to simulate the behaviour of a part with different materials, by applying different hydrostatic pressures. Large strainswere found in some cases, as the process reached the final separation. Therefore, the fracture criteria were suggested to recognize the limited strain depended on hydrostatic stress [12, 13].

The idea of using counter pressure in the process of tube hydroforming began when the successful effects to enhance the manufacturing capabilities were recognized. Processes, such as sheet hydroforming, have been extensively studied using the counter pressure, and all have produced final products with higher quality. Numerical approaches were developed in order to predict the results of final product by using deep drawing method.It was identified that the path of the pressure limitation can be identified in order to avoid process failure [14, 15].Hydroforming was simulated and used to determine bulge shape, as loads were applied on the three central elements [16]. Bulging production is essential to yield a successful process without causing any failuresuch as bursting, necking, and wrinkling. Exceeding the internal pressure causes thinning, while exceeding the applied axial force causes wrinkling in the final product [17, 18]. The counter pressure was used as an important factor in the tube hydroforming in the two mould types, T-shape and Y-shape, which avoids the internal pressure from the critical value [19, 20].

This paper aims to developa control model for the tube hydroforming process in real time in order to prevent any kind of failure. The process is simulated in the software to test the initial data for bothT-shape andX-shape. The developed software in MATLAB software package needs the initial data such as tube measurements, material properties, maximum axial force and maximum pressure. The program is able to apply different kinds of the functions into the pressure and the axial force curves. The developed program in MATLAB is connected to SOLIDWORKS by using a VBA code in order to receive the measurements data of the tube automatically from the CAD model. The data of the force and the axial curves could be sent to the CAD model in order to apply a simulation on the tube. The results of the program are compared with experimental outcomes.

2. Methodology

The aim of this section is to calculate the thinning of the tube through the process as well as prediction of bulge shape.

2.1 Numerical analysis

In this section the outer and the inner radius of the tube is depicted by b and a respectively. Besides the initial thickness of the tube wall is shown by t_0. In the following calculations, the change in length of the tube is identified by x while uncompressed length is identified by x_0, as illustrated in Figure 1.
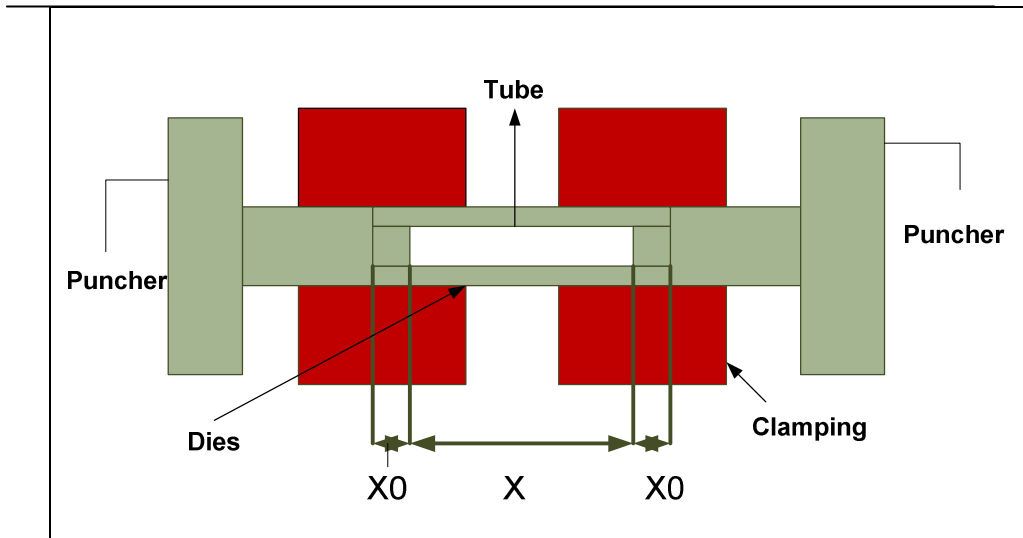
Figure1. The Schematic Model of a Tube Hydroforming System

In the following formula, the hoop strain is ignored in order to simplify the calculation modeling ($\varepsilon_\theta = 0$). Therefore, by initializing and with respect to the boundary conditions, the applied stress on the surface could be obtained by the following equation [21-23]:

$$\sigma_\theta(t) = \frac{1}{2}\left(\sigma_z(t) + \sigma_r(t)\right) \tag{1}$$

Where $\sigma_\theta(t)$, $\sigma_z(t)$ and $\sigma_r(t)$ are normal axial stress, axial stress and radial stress respectively. Besides, t is the time that varies the mentioned stress as a function of the time.

Furthermore, Equation 2 could be developed in order to force equilibrium in deformation zone in radial direction:

$$\frac{d\sigma_r}{dr} + \frac{-\sigma_\theta + \sigma_r}{r} = \frac{-2mk}{x} \tag{2}$$

Where, k is the constant friction and m is the demonstrated shear strength.

The applied radial stress on the inner wall is $\sigma_{ra} = p_i$ while p_i is the hydraulic pressure inside the tube. Therefore, applied axial stress (Z axis) on the inner wall could be calculated from Equation 3.

$$\sigma_{za}(t) = \sigma_{ra}(t) - \frac{2}{\sqrt{3}}\sigma_{yp}(t) = -P_i(t) - \frac{2}{\sqrt{3}}\sigma_{yp}(t) \tag{3}$$

The radial stress is calculated from Equation 4.

$$\sigma_{rb}(t) = -P_i(t) - \frac{\sigma_{yp}}{\sqrt{3}r}\ln\frac{a}{b} - \frac{2m\sigma_{yp}(a-b)}{\sqrt{3}x} - P_0(t) \tag{4}$$

The radial stress is utilized to calculate the normal axial stress on outer surface as shown in Equation 5.

$$\sigma_{zb}(t) = \sigma_{rb}(t) - \frac{2}{\sqrt{3}}\sigma_{yp} = -P_i(t) - \frac{\sigma_{yp}}{\sqrt{3}r}\ln\frac{a}{b} - \frac{2m\sigma_{yp}(a-b)}{\sqrt{3}x} - P_0(t) - \frac{2}{\sqrt{3}}\sigma_{yp} \tag{5}$$

The radial, normal axial and axial stress could be derived based on the stress diagram on the tube.
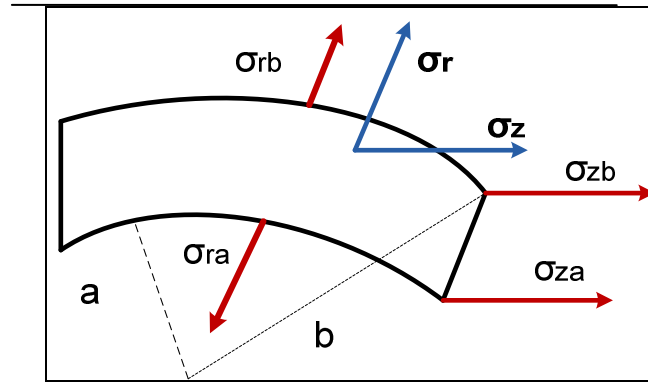
Figure2. The Applied Radial and the Axial Stress Diagram on the Tube

$$\sigma_r(t) = \sigma_{rb}(t) - \sigma_{ra}(t) \tag{6.a}$$

$$\sigma_z(t) = \frac{1}{2}\left(\sigma_{zb}(t) + \sigma_{za}(t)\right) \tag{6.b}$$

$$\sigma_\theta(t) = \frac{1}{2}\left(\sigma_z(t) + \sigma_r(t)\right) \tag{6.c}$$

The effective stress in the deformation region is derived using the VonMisses formulation shown in Equation 7.

$$\bar{\sigma}(t) = \frac{1}{\sqrt{2}}\left[\left(\sigma_r(t) - \sigma_\theta(t)\right)^2 + \left(\sigma_\theta(t) - \sigma_z(t)\right)^2 + \left(\sigma_z(t) - \sigma_r(t)\right)^2\right]^{1/2} \tag{7}$$

By using the obtained value, the effective strain could be calculated as:

$$\bar{\sigma}(t) = K\bar{\varepsilon}(t)^n \tag{8}$$

The effective strain could also be calculated using the VonMisses formulation as shown in Equation 9.

$$\bar{\varepsilon}(t) = \frac{2}{3}\left(\varepsilon_\theta(t)\right)^2 + \varepsilon_t(t)^2 + \varepsilon_z(t)^2) \tag{9}$$

The strain in radial direction is identified based on the initial assumptions($\varepsilon_\theta = 0$, $\varepsilon_t = -\varepsilon_z$).
Therefore the thickness of the tube could be determined by using Equation 10.

$$\varepsilon_t(t) = ln\frac{t_i(t)}{t_0(t)} \tag{10}$$

2.2 Simulation Study
In this section, the tube hydroforming and the dual hydroforming processes are simulated in the developed software [24]. The constant axial force and the change in the inner pressure are the boundary conditions of the following study. The non-linear dynamic simulation is developed for the processsscience the THF process demonstrates highly non-linear behaviour due to the occurrence of strain hardening and complex geometry as a result of the plastic deformation.
In the following simulations, the applied pressure ranges from 40 MPa to 60 MPa while the axial force is 48 KN throughout the simulations. The results shown in figures 3 to 6, demonstrate the applied stress and the deformation of T-shape and X-shape tubeswhile 50 MPa pressure is being applied inside the tube. Table 1 demonstrates the material and the tube properties.

Table1. The material properties and dimensions of the Aluminium tubeused for the process

	Tube Properties	
D	Outer Diameter	13.43 mm
ti	Thickness	1.37 mm
L	Length	107mm
	Material properties	
E	Youngs Modulus	70 GPa
ρ	Density	$2700 \ kg/m^3$
K	Strength Index	533.13 MPa
n	Strain Hardening	0.2837
υ	Poisson's Ratio	0.33
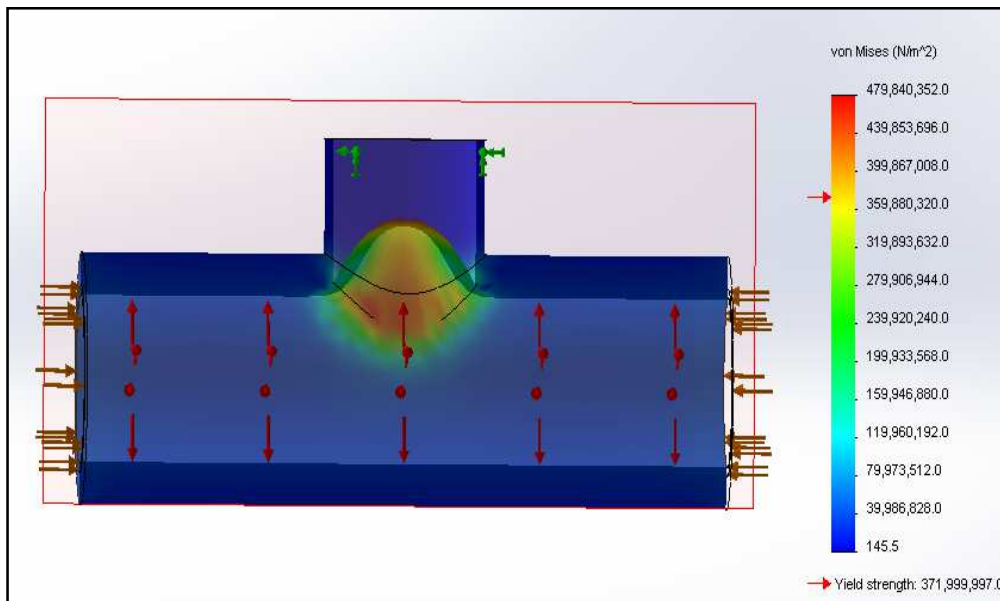
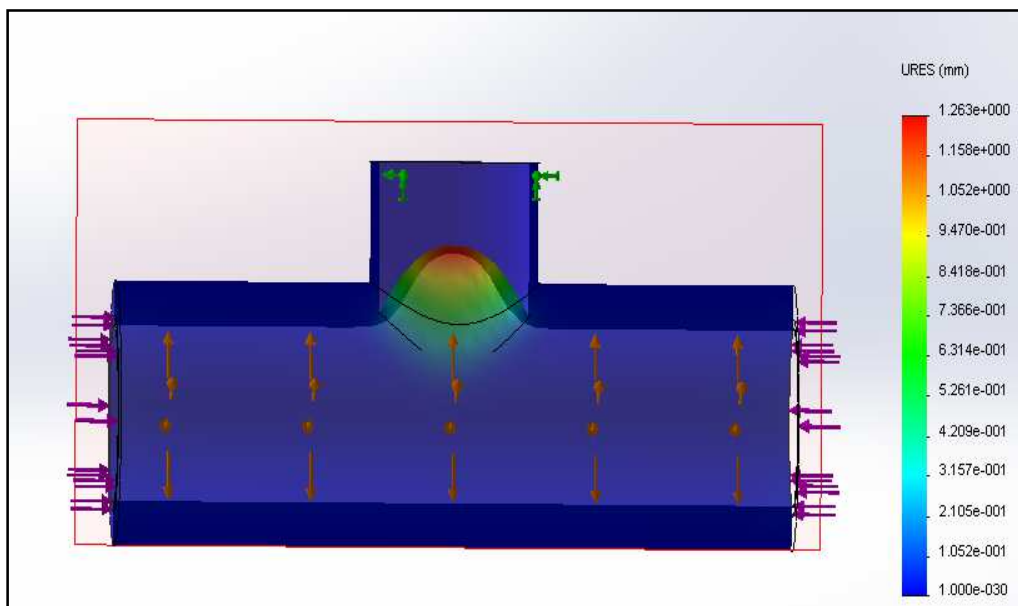Figure3. Applied Stress in the T-Shape Tube Hydroforming, Inner Pressure 50 Mpa

Figure4. Deformation in the T-Shape Tube Hydroforming, Inner Pressure 50 Mpa
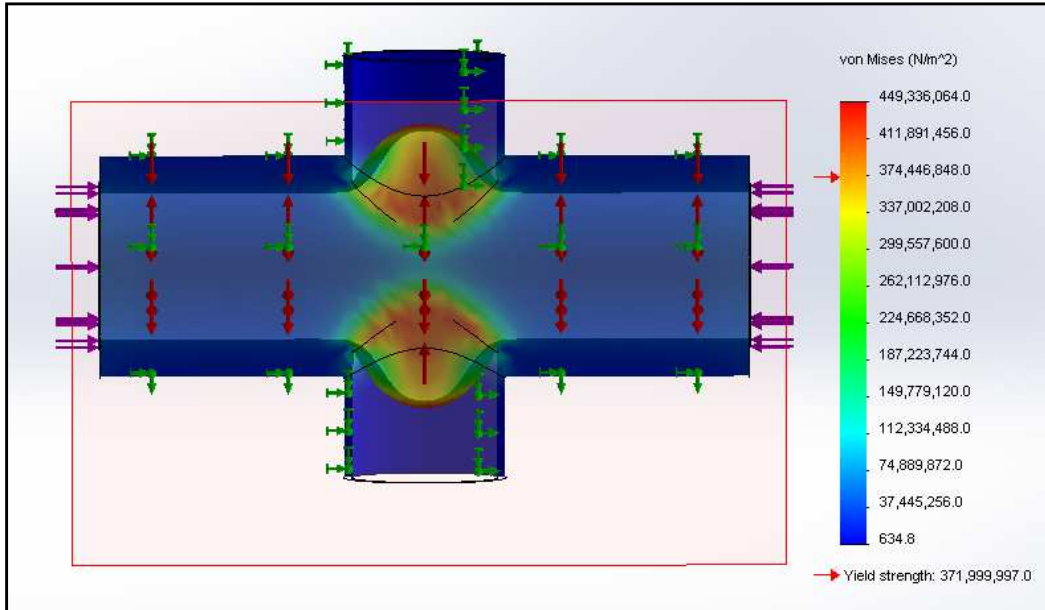
Figure5. Applied Stress in the X-Shape Tube Hydroforming, Inner Pressure 50 Mpa
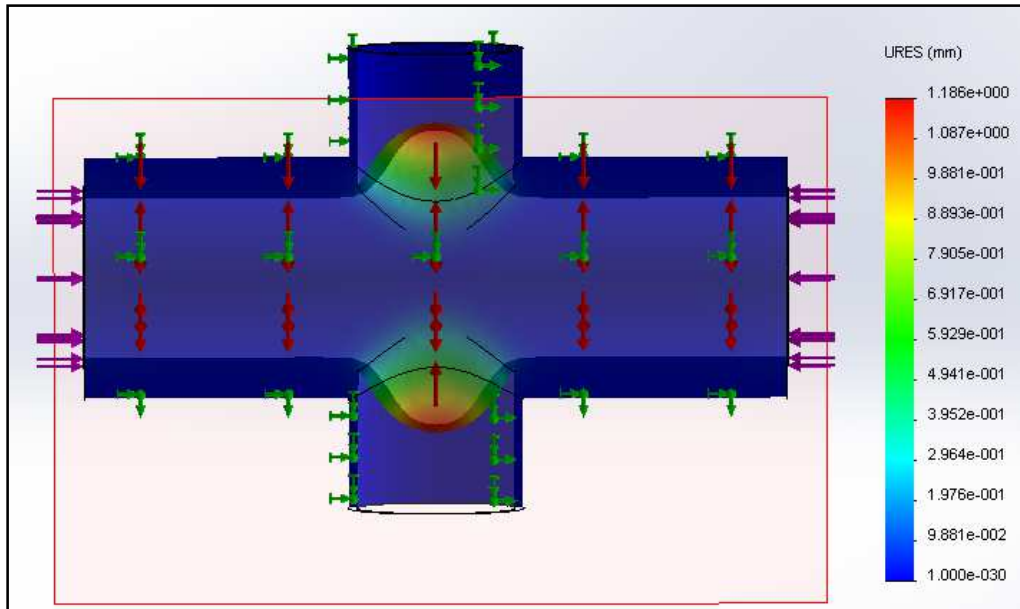

Figure6. Deformation in the X-Shape Tube Hydroforming, Inner Pressure 50 Mpa

For both produced tubes, the amount of deformation in first instant of the process has a linear function by increasing the inner pressure,as demonstrated in Figure 7,while increasing axial force causes different functionsas shown in Figure 8.The following figures comparisons of the static simulation for T-shape and X-shape while the hydroforming and dual hydroforming applied on the tube. The pressure range is between 45Mpa to 60 Mpa while the axial force is constant 48 kN in Figure 7. The axial range is 48 kN to 70 kN while pressure is constant in value of 50 Mpa. The following graphs are the results of the several simulations which are collected and demonstrated.
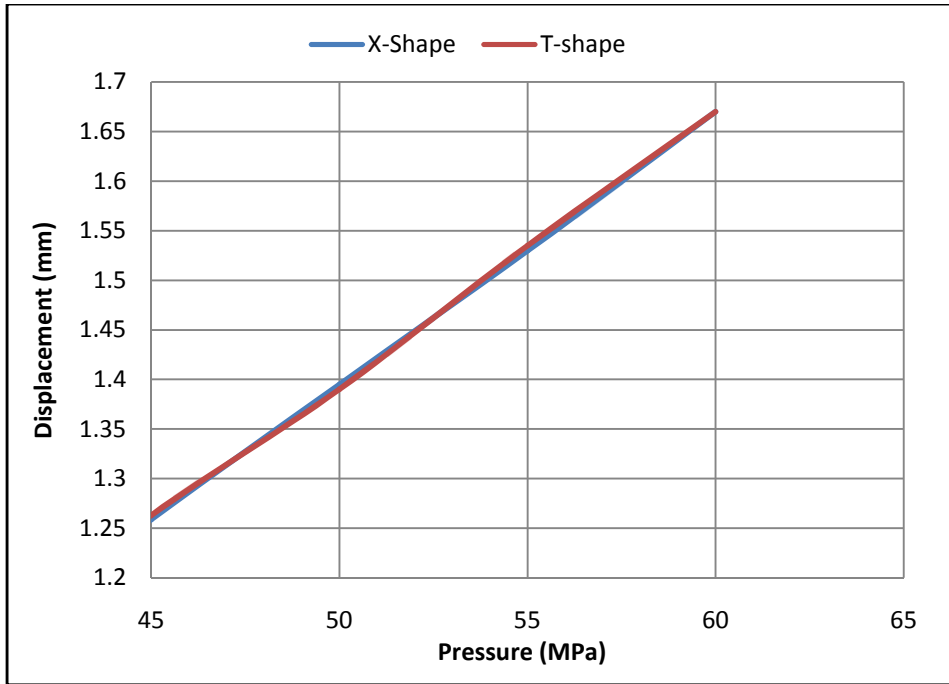
Figure7. Effect of the Pressure Changes Comparison in T-Shape and X-Shape in Hydroforming Process
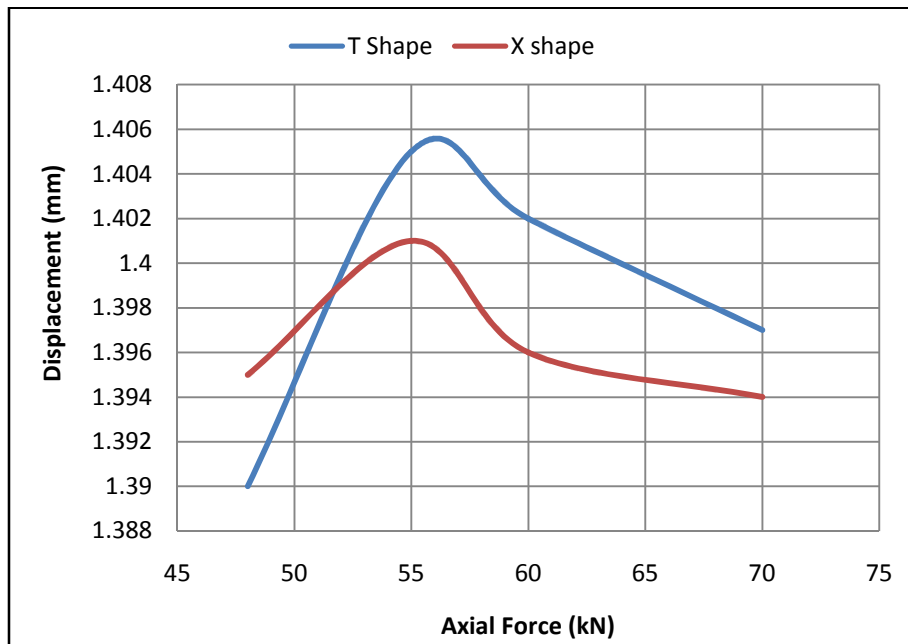

Figure8. The Effect of Changes in Axial Force Comparison in T-Shape and X-Shape in the Hydroforming Process

3. Control strategy development

The control strategy is developed in MATLAB software in order to manage the measurement of the axial force and the inner pressure. The tube properties such as the measurements and the material are the most important data required to be input in the software. The developed strategy is demonstrated in Figure 9.
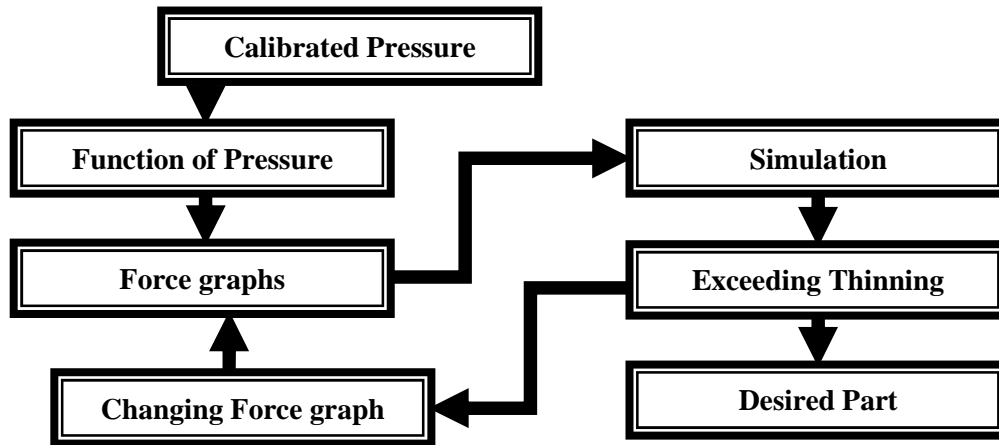
Figure9. The Control strategy applied to the Software

The developed CAD software is programmed to automatically input the tube material. The applied pressure and the axial force could be generatedthrough functions while the hydroforming and the dual hydroforming could be selected in the process simulation section.

The developed program is demonstrated in Figure 10 and the physical model is demonstrated in Figure 11.
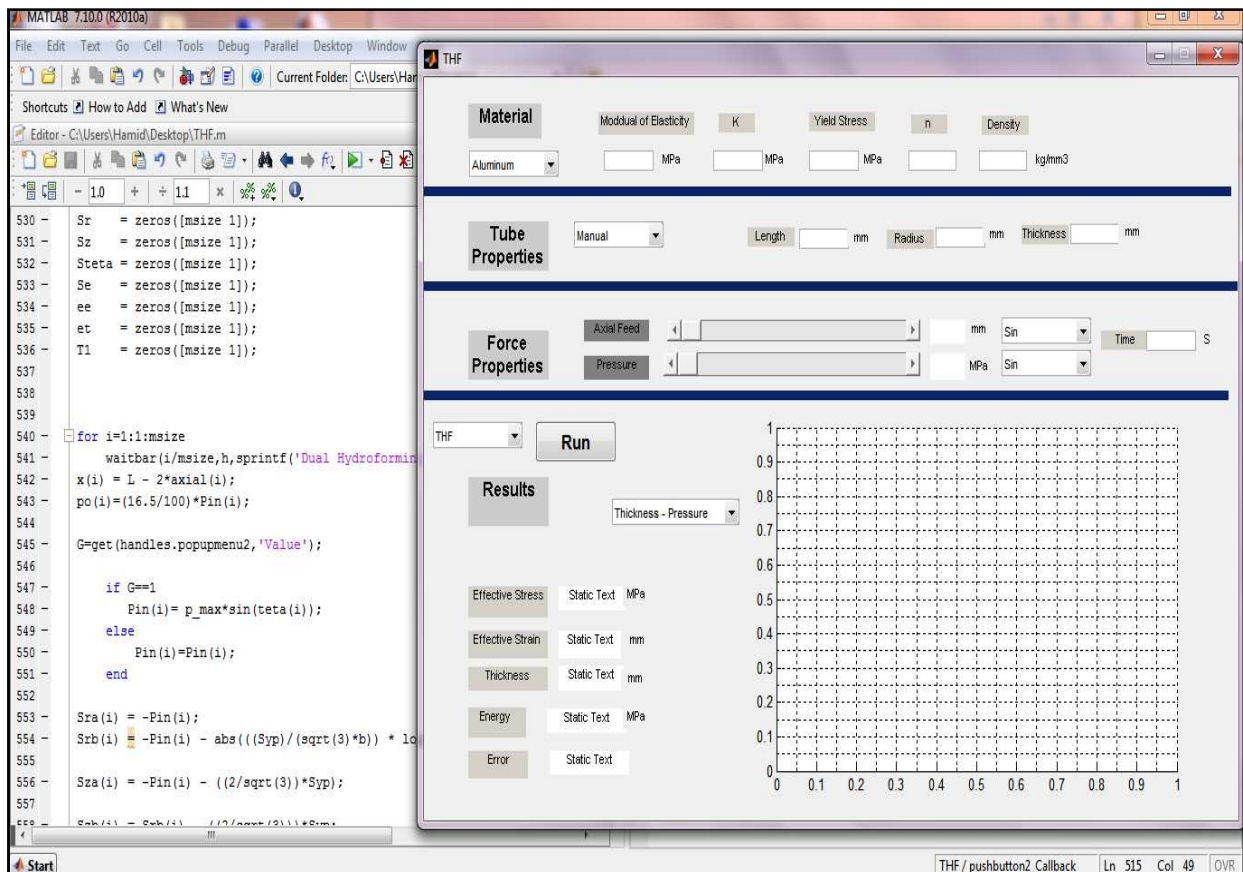

Figure10. The User Interface of the Developed Matlab Program

The high flexibility of the developed program allows a user to examine the process of tube hydroforming under different conditions.
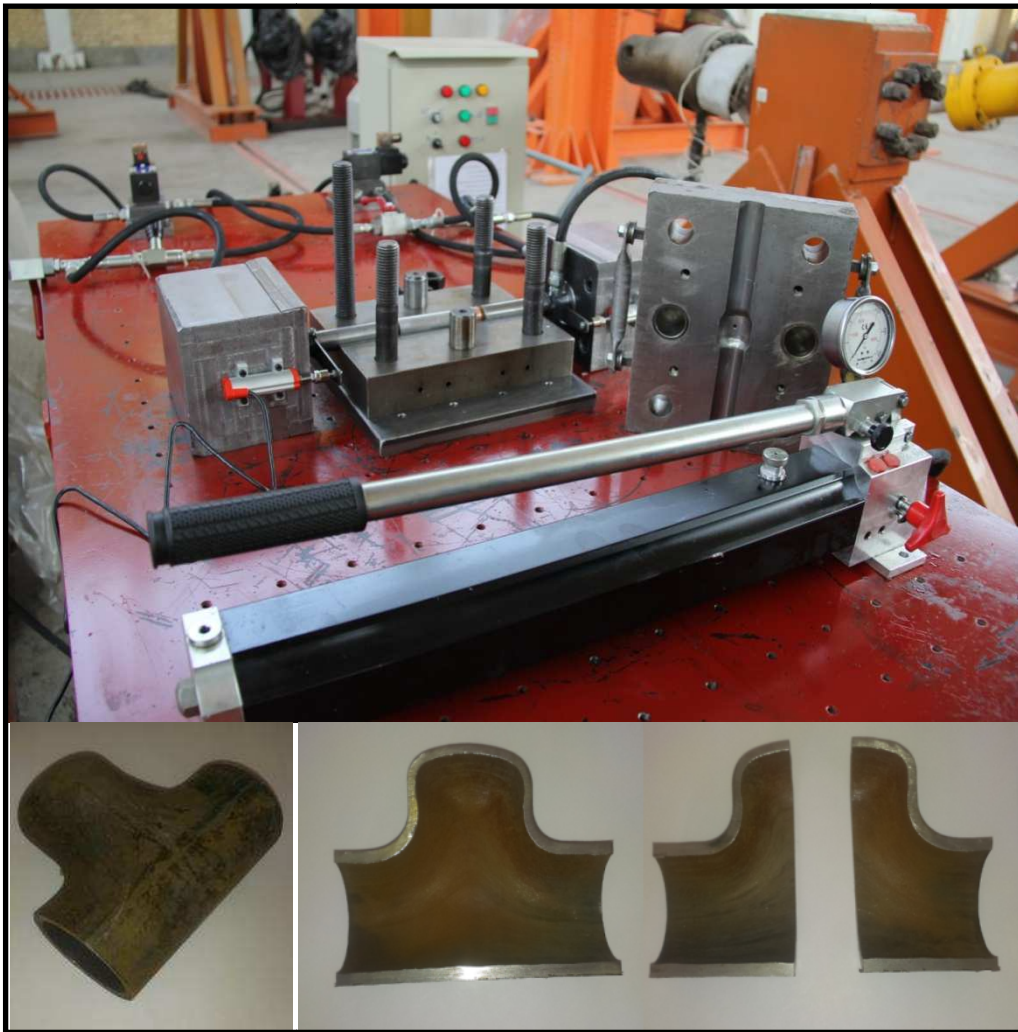
Figure11. The Developed Physical Hydroforming Machine

4. Results and discussion

The obtained results are measured for a particular tube with its length, thickness and outer radios predefined as 107 mm, 1.37 mm and 13.43 respectively. Furthermore, the inner pressure and the axial feed are assumed50Mpa and 20 mm respectively.

The change of the thickness in terms of the pressure is depicted in Figure 12. The test based on the mentioned conditions is carried out and simulated for tube hydroforming and dual hydroforming.
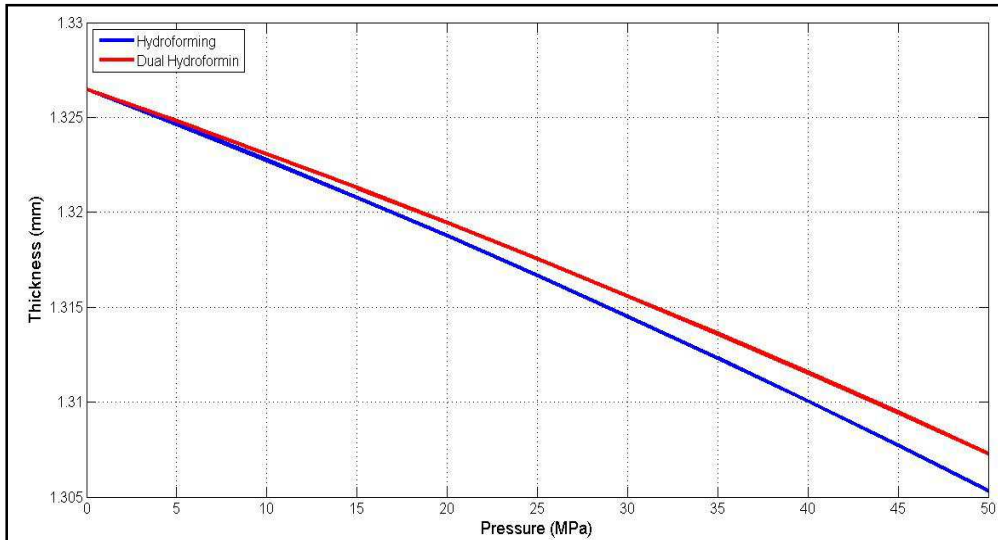
Figure12. The Changes of the Thickness through the Process

The thickness of the tube reduced more in the tube hydroforming compared to the dual hydroforming as shown in Figure 12. The obtained results successfully emulatedthe same outcomes of the experimentation in the other research.

The amount of the stress applied on the deformation zone is calculated for both types of the hydroforming process as shown in the Figure 13. The applied stress in dual hydroforming process is less than the traditional process. Therefore, from the results, it is evident that the dual hydroforming process is more efficient.
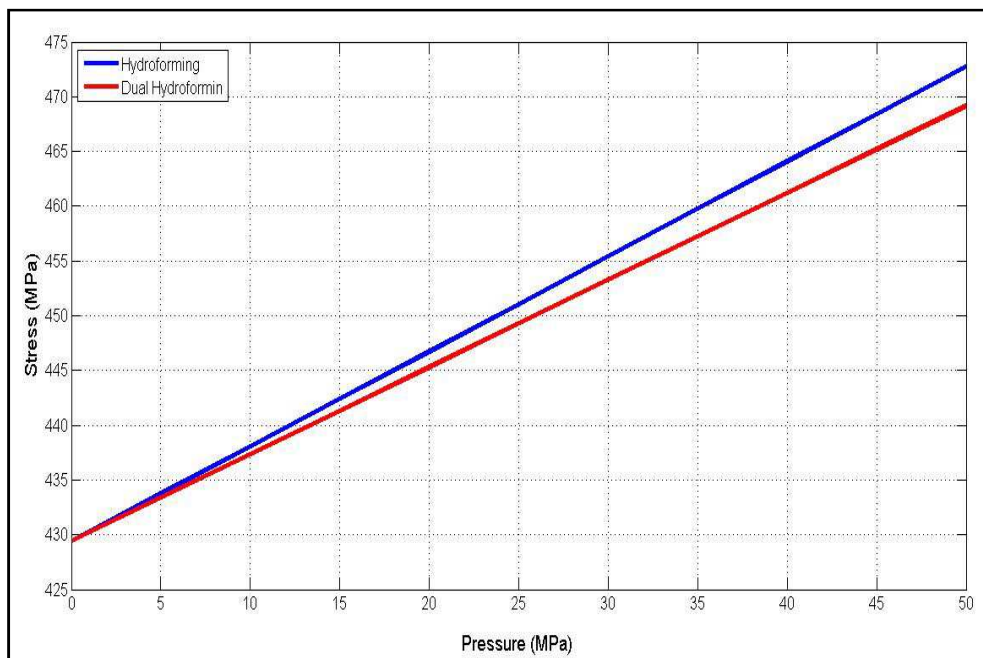

Figure13. The Applied Stress on the Deformation Zone

The amount of energy through the process is demonstrated in the Figure 14. The graph shows the comparisons of the mentioned type of the process.
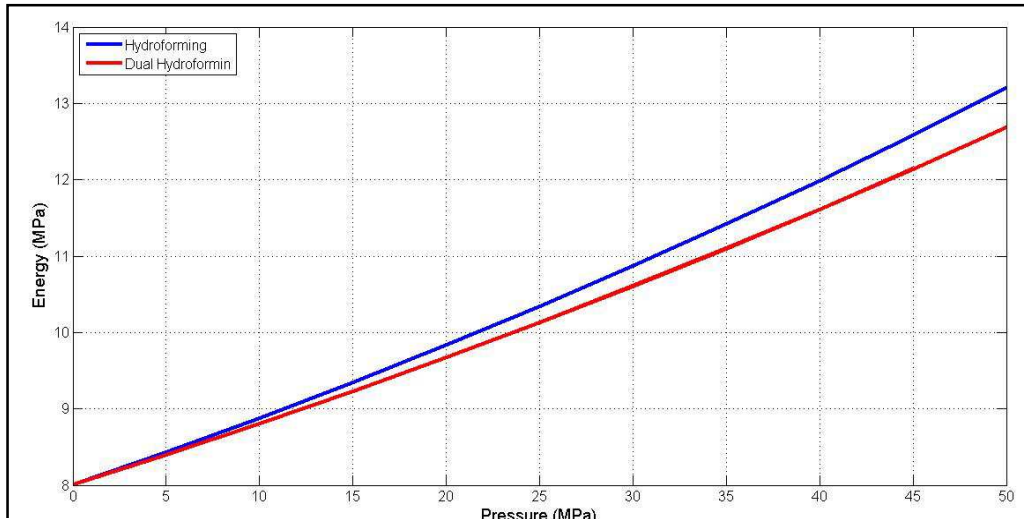
Figure14. Energy Needed for Deformation of the Tube

The obtained results for the change in thickness through the process, utilizing different tube materials are shown in Figure 15. The purpose of the following result is to study the effect of the tube martial on the process [25].
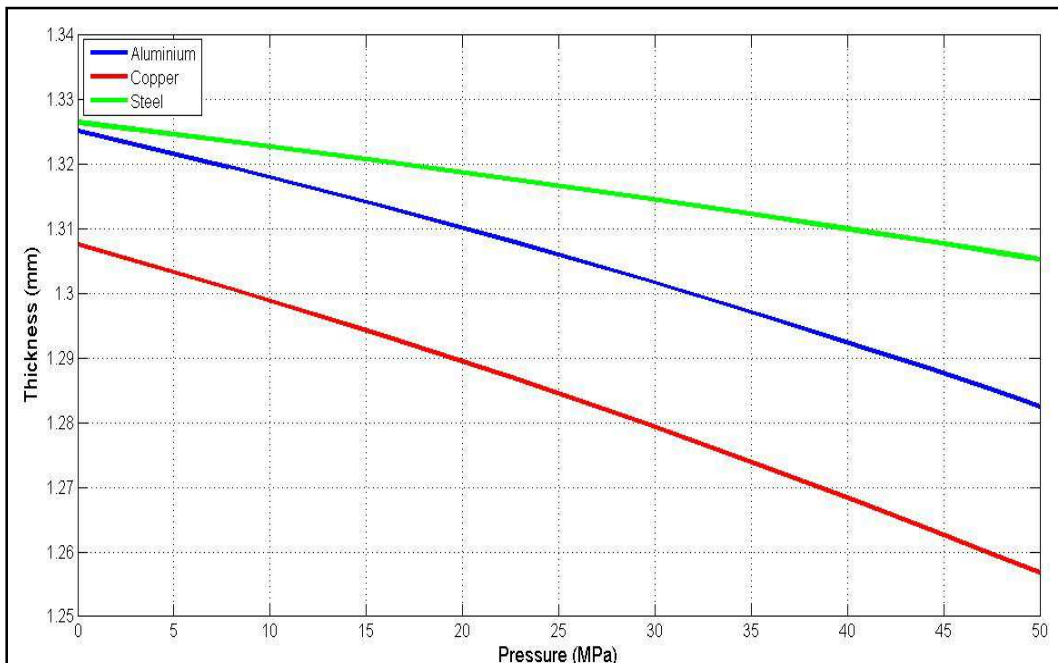
Figure15. The Effect of the Tube Material on the Tube Thickness

The same assumptions of experiment have applied for all the simulations, it is concluded that reduction in thickness is more efficient when using steel. However, due to steel properties, the amount of the energy needed for the process is much higher than other materials. The obtained data from the simulation are compared to the data from other resources. The simulation results were in accordance with the experiment results as shown in Table 2.

Table2. Comparisons of the Obtained Data of Simulation and Experiment

Inner Pressure (MPa)	Displacement (mm)		Thinning (%)	
	Experiment[46]	Simulation	Experiment	Simulation
35.4	8.5	8.46	3	2.48
41.4	10	11.17	7	7.59
48.3	11.5	11	12	11.68

The results of experiment and simulation are successfully matched. The error existed between the results of the experiment and simulation is suggested due to value of the friction coefficient which is neglected in the simulation.

5. Conclusion

This paper aimed to develop software for the hydroforming process of a tube. The developed program is able to analyze the process of hydroforming and dual hydroforming of the tube. The initial data of the program is tube sizes and material property. The program is able to automatically read the data of the tube size directly from the CAD model by using the developed VBA cod. The results of the pressure and axial force curves are sent to SOLIDWORKS in order to test static simulation on the tube based on the selected dies. The developed software is able to calculate the value of thinning of the tube wall through the process. The several static simulations are developed in order to investigate the effects of axial force and pressureexceeding on the result of displacement. The obtained results from the software are compared and matched with experimental outcomes.

6. References

[1] MalekzadehFard, K., Karami, J. and Nourifar, E. 2014. Hydroforming for Advanced Manufacturing, 1st edition, 17- 27.

[2] Bihamta, R. 2011. Optimisation of the Hydroforming Process of Geometrically Complex Aluminium Tubes Taking Account of Preceding Forming Processes, PhD thesis, University Laval Québec.

[3] Ray, P. 2005. Computer Aided Optimization of Tube Hydroforming Processes, Thesis of Doctor of Philosophy, Dublin City University.

[4] Dohmann, F. and Hartl, C. 1997. Tube Hydroforming Research and Practical Application, Journal of Materials Processing Technology, 71(1), 174-186.

[5] Ahmed, M. and Hashmi, M.S.J. 1998. Finite element analysis of bulge forming applying pressure and in-plane compressive load, Journal of Material Processing Technology, 77, 95-102.

[6] Limb, M., Chakrabarty, J., Garber, S. and Mellor, P .B. 1973. The forming of axisymmetric and asymmetric components from a tube, Proc. 14th International MTDR Conference, 799.

[7] Lukanov, V.L., Klechkov, V.V., Shateev, V.P. and Orlov, L.V. 1980. Hydromechanical Stamping of Tees with Regulated Liquid Pressure", Forging and Stamping Industry, 3(5-7), 181-185.

[8] Yang, J.B., Jeon, B.H and Oh, S.I. 2001. The Tube Bending Technology of a Hydroforming Process for an Automotive Part, Journal of Materials Processing Technology, 111, 175-181.

[9] Rimkus, W., Bauer, H. and Mihsein, M.J.A. 2000. Design of load curves for hydroforming applications, Journal of Materials Processing Technologies, 108, 97-105.

[10] Lejeune, A., Boudeau, N. and Gelin, J. C. 2003. Influence of material and process parameters on bursting during hydroforming process, Journal of Materials Processing Technology, 143-144, 11-17.

[11] Tirosh, J., Neuberger, A. and Shirizly, A. 1996. On tube expansion by internal fluid pressure with additional compressive stress, International Journal of Mechanical Sciences, 38(8), 839-851.

[12] Nefussi, G. and Combescure, A. 2002. Coupled buckling and plastic instability for tube hydroforming, International Journal of Mechanical Sciences, 44, 899-914.

[13] Ko, M. and Altan, T. 2002. Prediction of forming limits and parameters in the tube hydroforming process, International Journal of Machine Tools and Manufacture, 42, 123-133.

[14] Kocanda, A. and Sadlowska, H. 2008. Automotive component development by means of hydroforming, Archives of Civil and Mechanical Engineering, 8(3), 55–72.

[15] Wang, X.S., Yuan, S.J., Huang, X.R., Yao, Y.X. and Wang, Z.R. 2008. Research On Hydroforming Tubular Part With Large Perimeter Difference", Acta Metall. Sin. (Engl. Lett.), 21(2), 133-138.

[16] Kim, S. and Kim, Y. 2002. Analytical study for tube hydroforming , Journal of Material Processing Technology, 128, 232-239.

[17] Asnafi, N. 1999. Analytical modelling of tube hydroforming, Thin-Walled Structures, 34, 295-330.

[18] Ahmed, M. and Hashmi, M. S. J. 1999. Finite element simulation of bulge forming of an elbow of box section from circular tube, Journal of Materials Processing Technology, 92-93, 410-418.

[19] MacDonald, B.J. and Hashmi, M.S.J. 2000. Finite element simulation of bulge forming of a cross-joint from a tubular blank, Journal of Material Processing Technology, 103, 2000, 333-342.

[20] Koc, M., Allen, T., Jiratheranat, S. and Altan, T. 2000. The use of FEA and design of experiments to establish design guidelines for simple hydroformed parts, International Journal of Machine Tools & Manufacturing, 40, 2249-2266

[21] Jain, N. 2003. Modeling and Analysis of Dual Hydroforming Process, Thesis of Master of Science, Submitted to Texas A&M University.

[22] Xing, H.L. and Makinouchi, A. 2001. Numerical analysis and design for tubular hydroforming, International Journal of Mechanical Sciences, 43 , 1009-1026.

[23] Cherouat, A., Saanouni, K. and Hammi, Y. 2002. Numerical improvement of thin tubes hydroforming with respect to ductile damage, International Journal of Mechanical Sciences, 44, 2427–2446.

[24] Hwang, Y.M and Altanb, T. 2002. Finite element analysis of tube hydroforming processes in a rectangular die, Finite Elements in Analysis and Design, 39, 1071–1082.

[25] Alaswa, A., Benyounis, K.Y. and Olabi, A.G. 2012. Tube hydroforming process: A reference guide, Materials and Design, 33, 328–339.